Stability of biaxial nematic phase for systems with variable molecular shape anisotropy

Lech Longa,[1,2,*] Grzegorz Pająk,[1] and Thomas Wydro[1,2,†]
[1]*Marian Smoluchowski Institute of Physics, Department of Statistical Physics and Mark Kac Center for Complex Systems Research, Jagiellonian University, Reymonta 4, Kraków, Poland*
[2]*Laboratoire de Physique Moléculaire et des Collisions, Université Paul Verlaine-Metz, 1 bvd Arago, 57078 Metz, France*
(Received 8 December 2006; published 13 July 2007)

We study the influence of fluctuations in molecular shape on the stability of the biaxial nematic phase by generalizing the mean-field model of Mulder and Ruijgrok [Physica A **113**, 145 (1982)]. We limit ourselves to the case when the molecular shape anisotropy, represented by the alignment tensor, is a random variable of an annealed type. A prototype of such behavior can be found in lyotropic systems—a mixture of potassium laurate, 1-decanol, and D_2O, where distribution of the micellar shape adjusts to actual equilibrium conditions. Further examples of materials with the biaxial nematic phase, where molecular shape is subject to fluctuations, are thermotropic materials composed of flexible trimericlike or tetrapodlike molecular units. Our calculations show that the Gaussian equilibrium distribution of the variables describing molecular shape (dispersion force) anisotropy gives rise to new classes of the phase diagrams, absent in the original model. Depending on properties of the shape fluctuations, the stability of the biaxial nematic phase can be either enhanced or depressed, relative to the uniaxial nematic phases. In the former case the splitting of the Landau point into two triple points with a direct phase transition line from isotropic to biaxial phase is observed.

DOI: 10.1103/PhysRevE.76.011703 PACS number(s): 61.30.Cz, 64.70.Md

I. INTRODUCTION

The biaxial nematic phase is one of the perennially challenging problems of experimental soft matter physics. Although predicted theoretically by Freiser in 1970 [1] it was not until 1980 that the first experimental observation of this phase has been reported [2]. The phase was discovered in a lyotropic, ternary mixture of potassium laurate, 1-decanol, and D_2O and its stability attributed to shape change of the micellar aggregates as a function of temperature and concentration of amphiphilic molecules [3]. The search for a thermotropic biaxial nematic has proved highly controversial for more than two decades. A first qualitative report on a stable uniaxial-to-biaxial nematic phase transition has been reported by Li *et al.* [4] in their system of flexible, ring-shaped trimeric liquid crystal. Recently, this phase has also been detected in two classes of thermotropic materials. It was reported in "banana-shaped" mesogens [5,6] and in liquid crystalline tetrapodes [7]. The last class of materials is particularly interesting for it comprises molecules with four mesogenic units connected together through a flexible spacer. The optimal packing of such tetrapodes in the biaxial nematic phase is achieved for a quasiflat, platelet configuration of the tetrapod's mesogens that are, on the average, tilted in the plane of the platelet.

A challenge for theory is to find molecular factors responsible for absolute stability of the observed biaxial nematic phase. The presently existing microscopic models [1,8–11] show that the molecular shape and pair interaction biaxiality are obviously important for the biaxial phase to exist. However, as numerous experimental reports have demonstrated [12], they seem not sufficient to get the absolutely stable biaxial phase. In the present paper we show that a variable (fluctuating) anisotropy of the molecular shape can be an important stabilizing factor for this phase to occur. Indeed, it seems that this factor appears commonly in the micellar, trimeric, and tetrapod systems. Let us mention that the theoretical studies and computer simulations so far have addressed the size and shape of the micelles in lyotropic systems [13–16], but a connection between the shape anisotropy distribution and the stability of the biaxial nematic phase have not yet been explored.

The present paper is arranged as follows. After the introduction of the model in Sec. II, we explore stability of the biaxial nematic phase on shape fluctuations in Sec. III. Section IV is devoted to a short summary.

II. THE MODEL

We assume that the Hamiltonian $H(\{\mu\},\{\mathbf{S}\})$ of N liquid crystalline molecules with dynamical degrees of freedom $\{\mathbf{S}\}$ also depends on the $\{\mu\}$ variables, which parametrize molecular shape. The partition function is calculated for each allowed configuration of randomly chosen $\{\mu\}$. Then, in analogy to statistics of disordered systems with annealed disorder [17], $\{\mu\}$ is treated as a set of dynamical variables that adjust to actual equilibrium conditions. Under these circumstances the free energy, F, of the system can be approximated by the logarithm of the $\{\mu\}$ averaged partition function,

$$F = -k_B T \ln Z, \tag{1}$$

$$Z = \sum_{\{\mu\}} P(\{\mu\}) \sum_{\{\mathbf{S}\}} e^{-\beta H(\{\mu\},\{\mathbf{S}\})}, \tag{2}$$

where $P(\{\mu\})$ is the probability distribution of the $\{\mu\}$ variables. A role played by the distribution P on the formation of the biaxial nematic phase is studied by generalizing a very

*Electronic address: longa@th.if.uj.edu.pl
†Electronic address: wydro@univ-metz.fr

elegant mean-field model of Mulder and Ruijgrok [8] (MR), which employs a connection between the SU(3) symmetry and the biaxial nematic liquid. The most important feature of the model is that its partition function can be calculated exactly, which, as we are going to show, allows one for a semianalytical treatment of the annealed average (2). More specifically, in the MR model the internal, dynamical state of each molecule is parametrized by eight degrees of freedom: three components L_α of the angular momentum $\mathbf{L}$ and five components $Q_{\alpha\beta}$ of the symmetric and traceless quadrupole moment $\mathbf{Q}$. These eight variables are next combined to form eight generators S_a of the SU (3) algebra, establishing equivalence between $\{\mathbf{L},\mathbf{Q}\}$ and $\mathbf{S}=\Sigma_{a=1}^{8} S_a \boldsymbol{\lambda}_a$, where $\boldsymbol{\lambda}_a$ are the Gell-Mann matrices: $(\mathbf{S})_{\alpha\beta}=Q_{\alpha\beta}-\frac{i}{2}\Sigma_\gamma \varepsilon_{\alpha\beta\gamma} L_\gamma, \alpha,\beta,\gamma=1,\ldots,3$. The MR Hamiltonian is the mean-field (MF) version of the Heisenberg-type interaction [8]

$$H \equiv H_{\mathrm{MF}} = \frac{JN}{4}\mathrm{Tr}(\bar{\mathbf{S}}\bar{\mathbf{S}}) - \frac{J}{2}\sum_{i=1}^{N}\mathrm{Tr}(\bar{\mathbf{S}}\mathbf{S}_i), \tag{3}$$

where the dynamical variables $\mathbf{S}_i$ are subject to two i-independent constraints, represented by Casimir invariants of the SU(3) algebra

$$\mathrm{Tr}(\mathbf{S}_i^2) = \mathrm{Tr}(\tilde{\mathbf{Q}}_i^2) = \sum_{\alpha=1}^{3}\mu_{i,\alpha}^2 = 2I_2(\boldsymbol{\mu}_i), \tag{4}$$

$$\mathrm{Tr}(\mathbf{S}_i^3) = \mathrm{Tr}(\tilde{\mathbf{Q}}_i^3) = \sum_{\alpha=1}^{3}\mu_{i,\alpha}^3 = 2I_3(\boldsymbol{\mu}_i), \tag{5}$$

with $\mu_{i,1}+\mu_{i,2}+\mu_{i,3}=0$; N is the number of molecules and $\bar{\mathbf{S}}$ is the thermodynamic average of $\mathbf{S}_i$. The $\mu_{i,\alpha}$ variables are the eigenvalues of the traceless matrices $\mathbf{S}_i$, or $\tilde{\mathbf{Q}}_i$, where $\tilde{\mathbf{Q}}_i$ is the quadrupole moment of the ith molecule at rest ($\mathbf{L}_i=0$), obtained from $\mathbf{S}_i$ by applying an SU(3) transformation. Hence, if $\tilde{\mathbf{Q}}_i$ represents, e.g., the quadrupole moment of a mass distribution the intrinsic properties of a given molecule, like the ratios of its principal axes, enter through the Casimir invariants $I_2(\boldsymbol{\mu}_i)$, $I_3(\boldsymbol{\mu}_i)$, Eqs. (4) and (5). This remains in full analogy with what we practice for an ordinary quadrupolar tensor, where the I_2- and I_3-like invariants are used to characterize biaxiality of a relevant physical observable [18,19]. More specifically, depending on the values of I_2 and I_3, or their ratio

$$w = \sqrt{3}\frac{I_3}{(I_2)^{3/2}}, \tag{6}$$

three possibilities can be distinguished: (a) for $I_2=I_3=0$ the tensor is isotropic; (b) for $3I_3^2=I_2^3$ the tensor is uniaxial; and (c) for $3I_3^2<I_2^3$ the tensor is biaxial with maximal biaxiality being obtained for $I_3=0$. The sign of I_3 decides about whether the tensor is prolate (plus sign) or oblate (minus sign). Respectively, $w=1$ ($w=-1$) and $|w|<1$ refers to rodlike (disklike) and biaxial molecules. By construction the MR model is SU(3) invariant with degrees of freedom running over the group manifold and its free energy is given in an analytical form as derived by Itzykson and Zuber [20].

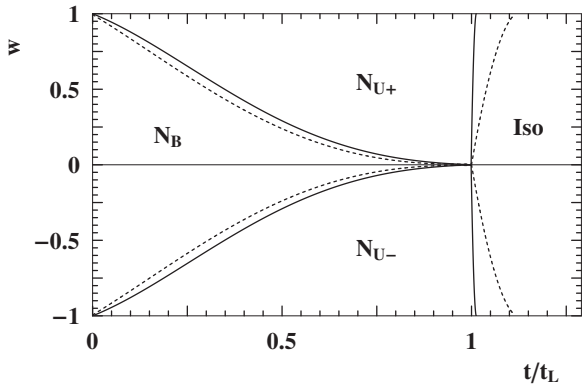

FIG. 1. Comparison of the MR phase diagram [8] (continuous lines) with one calculated for the Luckhurst *et al.* dispersion model [21,22] (dashed lines); $-1\le w=\sqrt{6}\,\mathrm{Tr}(\hat{\mathbf{R}}^3)=[(1-6\kappa^2)/(1+2\kappa^2)^{3/2}]\le 1$.

From physical point of view the model matches the standard Landau-de Gennes phase diagram for biaxial nematics [18], known to characterize systems with purely dispersion-type interactions. It also reproduces the mean-field results for the dispersion model of Luckhurst *et al.* [21,22], Fig. 1, given that we take the pair interactions of the form $V=-\epsilon\,\mathrm{Tr}(\hat{\mathbf{R}}\,\hat{\mathbf{R}}')$, where $\hat{\mathbf{R}}$ denotes the normalized quadrupole tensor ($\mathrm{Tr}\,\hat{\mathbf{R}}^2=1$) defined through the relation $\sqrt{1+2\kappa^2}\hat{\mathbf{R}}=\frac{1}{\sqrt{6}}(3\hat{\mathbf{z}}\otimes\hat{\mathbf{z}}-\mathbf{1})\pm\kappa(\hat{\mathbf{x}}\otimes\hat{\mathbf{x}}-\hat{\mathbf{y}}\otimes\hat{\mathbf{y}})$; κ is the ratio of biaxial-to-uniaxial polarizability of the molecule. The relative error for the N_U-N_B boundary calculated for both models does not exceed 2% and is even smaller for the nematic order parameter (see Fig. 4 in [8]). Note however the usefulness of the SU(3) symmetry. It avoids calculation of integrals over Euler angles inherent to the dispersion model, which, in turn, allows for comprehensive studies of flexible quadrupoles.

A generalization of the MR model to systems with variable anisotropy of the molecular shape (dispersion forces) is straightforward. We assume that $\mu_{i,1}$ and $\mu_{i,2}$ are annealed degrees of freedom weighted with the probability $P(\mu_{1,1},\mu_{1,2},\mu_{2,1},\ldots,\mu_{N,2})\approx\Pi_{i=1}^{N}P(\mu_{i,1},\mu_{i,2})$. The mean-field partition function, $Z=Z_1^N$, and the dimensionless free energy are then given by

$$Z_1 = e^{-\mathrm{Tr}(\bar{\mathbf{S}}\bar{\mathbf{S}})/4t}Q, \tag{7}$$

$$Q = \left\langle \int d\mathbf{S}\, e^{\mathrm{Tr}(\bar{\mathbf{S}}\mathbf{S})/2t}\,\delta\!\left(\frac{\mathrm{Tr}(\mathbf{S}^2)}{2}-I_2(\boldsymbol{\mu})\right)\delta\!\left(\frac{\mathrm{Tr}(\mathbf{S}^3)}{2}-I_3(\boldsymbol{\mu})\right)\right\rangle, \tag{8}$$

$$F = -Nt\,\mathrm{In}\,Z_1, \tag{9}$$

where $t=k_BT/J$ is the dimensionless temperature and where $\langle\cdots\rangle=\int(\cdots)P(\mu_1,\mu_2)d\mu_1 d\mu_2$. According to Itzykson and Zuber [20] the integral over $\mathbf{S}$ in (8) can be carried out to give

$$Q = \frac{2}{\Delta_{\bar{\gamma}}}\left\langle \frac{D}{\Delta_{\boldsymbol{\mu}}} \right\rangle, \tag{10}$$

where

$$D = \det\begin{pmatrix} e^{\bar{\gamma}_1\mu_1} & e^{\bar{\gamma}_2\mu_1} & e^{\bar{\gamma}_3\mu_1} \\ e^{\bar{\gamma}_1\mu_2} & e^{\bar{\gamma}_2\mu_2} & e^{\bar{\gamma}_3\mu_2} \\ e^{\bar{\gamma}_1\mu_3} & e^{\bar{\gamma}_2\mu_3} & e^{\bar{\gamma}_3\mu_3} \end{pmatrix}, \tag{11}$$

and where

$$\Delta_{\mathbf{x}} = (x_1 - x_2)(x_2 - x_3)(x_3 - x_1). \tag{12}$$

The eigenvalues $\bar{\gamma}_\alpha$ of the traceless matrix $\bar{\mathbf{S}}/(2t)$, are determined from the minimum of the free energy (9). In analogy to (4) and (5) the invariants $I_2(\bar{\gamma})$ and $I_3(\bar{\gamma})$ are used to distinguish between (a) the isotropic phase $[I_2(\bar{\gamma})=I_3(\bar{\gamma})=0]$; (b) the uniaxial nematic phase $[3I_3(\bar{\gamma})^2=I_2(\bar{\gamma})^3]$; and (c) the biaxial nematic phase $[3I_3(\bar{\gamma})^2<I_2(\bar{\gamma})^3]$. In addition, $I_3(\bar{\gamma})$ is positive for the prolate uniaxial phase (N_{U+}) and negative for the oblate uniaxial phase (N_{U-}).

The annealed averaging $\langle\cdots\rangle$ over $P(\mu_1,\mu_2)$, Eq. (8), has a very simple interpretation in the mean-field theory. Setting $\bar{\gamma}_\alpha=0$ ($\alpha=1,2$), which is always one of the mean-field solutions, we find that $P(\mu_1,\mu_2)$ matches the density distribution of the molecular shape anisotropy in the reference (stable or metastable) disordered phase. We believe therefore that for a credible choice of $P(\mu_1,\mu_2)$ the model correctly reproduces generic phase behavior for flexible quadrupoles in the vicinity of the isotropic phase. Clearly, the original MR model is recovered if $P(\mu_1,\mu_2)$ is given by the Dirac delta distribution. In what follows we take P to be the Gaussian distribution. This choice is consistent with the maximum entropy principle applied in the isotropic phase and the observation that usually only the first two moments of P can be determined reasonably well from experiment [3]. Assuming that in the reference (disordered) phase these moments are given by $\langle\mu_\alpha\rangle=m_\alpha$, $\langle(\mu_\alpha-m_\alpha)^2\rangle=\sigma_\alpha^2$, and $\langle(\mu_1-m_1)(\mu_2-m_2)\rangle=\tilde{\lambda}\sigma_1\sigma_2$ ($\alpha=1,2$) we find

$$P(\mu_1,\mu_2) = \frac{\sqrt{a}}{2\pi\sigma_1\sigma_2} e^{-(1/2)\sum_{\alpha\beta}(\mu_\alpha-m_\alpha)\sigma_{\alpha\beta}(\mu_\beta-m_\beta)}, \tag{13}$$

where

$$\boldsymbol{\sigma} = \begin{pmatrix} \dfrac{a}{\sigma_1^2} & -\dfrac{\lambda}{\sigma_1\sigma_2} \\ -\dfrac{\lambda}{\sigma_1\sigma_2} & \dfrac{a}{\sigma_2^2} \end{pmatrix} \tag{14}$$

with λ being the real parameter, $a=\frac{1}{2}(1+\sqrt{1+4\lambda^2})$ and $-1\le\tilde{\lambda}=\frac{\lambda}{a}\le 1$. The distribution $P(\mu_3)$ of μ_3, obeying the constraint $\mu_1+\mu_2+\mu_3=0$, is also a Gaussian with average $\langle\mu_3\rangle=m_3=-m_1-m_2$ and dispersion $\sigma_3^2=\sigma_1^2+2\tilde{\lambda}\sigma_1\sigma_2+\sigma_2^2$ ($|\sigma_1-\sigma_2|\le\sigma_3\le\sigma_1+\sigma_2$), $P(\mu_3)=\frac{1}{\sqrt{2\pi}\sigma_3}\exp\left(-\frac{(\mu_3+m_1+m_2)^2}{2\sigma_3^2}\right)$. In general, the parameters of the distribution (13) can depend on temperature, but this possibility, which can be relevant for quantitative understanding of phase diagrams in lyotropic systems, will not be discussed here.

III. RESULTS

The phase diagrams, obtained from the global minimization of the free energy (9) with respect to $\{\bar{\gamma}_\alpha,\alpha=1,2\}$, depend on the values of five parameters: m_1, m_2, σ_1, σ_2, and λ (or σ_3) of the Gaussian distribution (13). To make a direct comparison with the earlier work [8] we use, instead of m_1 and m_2, the molecular shape parameter $w(\boldsymbol{m})$ and $I_2(\boldsymbol{m})$, Eqs. (4) and (6). A connection between the parametrizations is given by

$$m_1 + m_2 = u, \tag{15}$$

$$m_1 m_2 = u^2 - I_2, \tag{16}$$

where u is a solution of the cubic equation

$$u^3 - uI_2 + \frac{2\sqrt{3}}{9}(I_2)^{3/2}w = 0. \tag{17}$$

The three real roots $u_1\le u_2\le u_3$ of Eq. (17) correspond to different permutations between axes of the molecule-fixed frame. In what follows we choose the u_2 solution to identify the corresponding m_1 and m_2. Solving Eqs. (15) and (16) for given u_2 and I_2 still leaves a freedom to choose the pair $\{m_1,m_2\}$ up to a permutation. We select the solution for which $m_1\le m_2$. Permutation symmetry of Q: $Q(\{m_\alpha\},\{\sigma_\alpha\},\ldots)=Q(\{m_{\mathcal{P}(\alpha)}\},\{\sigma_{\mathcal{P}(\alpha)}\},\ldots)$, where $\mathcal{P}$ is an arbitrary permutation of $\{1,2,3\}$, allows us to construct the remaining diagrams for $m_1\ge m_2$ from the ones given.

Numerical calculations are carried out for fixed values of σ_1, σ_2, and λ. The phase diagrams are shown in plane with the molecular shape parameter $w(\boldsymbol{m})$ and the reduced temperature t/t_L, with $t_L\ge\frac{\langle I_2(\boldsymbol{\mu})\rangle}{8}$ being the isotropic-nematic transition temperature for $w(\boldsymbol{m})=0$. In all cases the numerical value of I_2 was fixed to $I_2=\frac{1}{4}$. The diagram for $I_2=\frac{1}{4}\xi^2$, σ_i, and λ, where ξ is an arbitrary real number, can be obtained from that for $I_2=\frac{1}{4}$, $\sigma_i\to\sigma_i/\xi$, and λ, which follows from invariance of Q, Eq. (8), with respect to ξ rescaling of the parameters: $Q(\{m_i\},\{\sigma_i\},\lambda,t)=Q(\{\xi m_i\},\{\xi\sigma_i\},\lambda,\xi t)$. In addition, the invariance of Q, Eq. (8), with respect to change of $\{\boldsymbol{\mu},\bar{\gamma}\}$ into $\{-\boldsymbol{\mu},-\bar{\gamma}\}$ makes the phase diagrams symmetric with respect to the line $w(\boldsymbol{m})=0$.

Numerical minimization of the free energy allows us to divide all of the diagrams into classes shown in Figs. 2–4. The corresponding isotropic-nematic transition temperature t_L is plotted in Figs. 5 and 6. At high temperatures, in the vicinity of isotropic-nematic phase transition, the results can be understood qualitatively from the expansion of Q, Eq. (10), about $\bar{\gamma}_i=0$. Up to sixth order in $\bar{\gamma}_i$ it reads

$$\begin{aligned} Q \approx 1 &+ \tfrac{1}{4}\langle I_2\rangle I_2(\bar{\gamma}) + \tfrac{1}{10}\langle I_3\rangle I_3(\bar{\gamma}) + \tfrac{1}{40}\langle I_2^2\rangle I_2(\bar{\gamma})^2 \\ &+ \tfrac{1}{70}\langle I_2 I_3\rangle I_2(\bar{\gamma})I_3(\bar{\gamma}) + \left(\tfrac{17}{12\,096}\langle I_2^3\rangle - \tfrac{1}{5040}\langle I_3^2\rangle\right)I_2(\bar{\gamma})^3 \\ &+ \left(\tfrac{1}{420}\langle I_3^2\rangle - \tfrac{1}{5040}\langle I_2^3\rangle\right)I_3(\bar{\gamma})^2 + \cdots, \end{aligned} \tag{18}$$

where the averages over $\boldsymbol{\mu}$ are given by

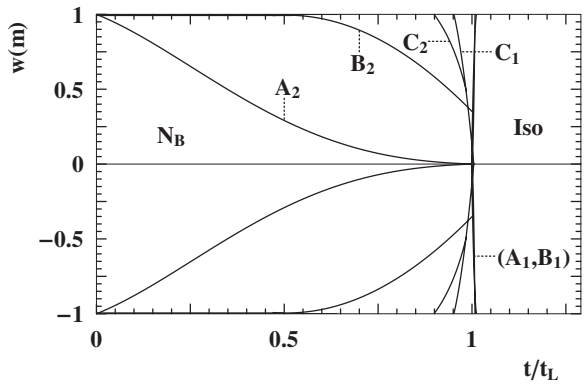

FIG. 2. Phase diagrams for $\sigma_2=0$. Diagrams labeled A_i, B_i, and C_i correspond to $\sigma_1=0$ [8], 0.15, and 0.3, respectively. Subscript $i=1$ refers to the isotropic (iso)nematics phase transition lines whereas subscript $i=2$ refers to the uniaxial nematic-biaxial nematic (N_B) lines.

$$\langle I_2\rangle = I_{20} + I_{02},$$

$$\langle I_3\rangle = I_{30} + 3I_{12},$$

$$\langle I_2^2\rangle = I_{20}^2 + 6I_{22} + 3I_{04},$$

$$\langle I_2 I_3\rangle = I_{20}I_{30} + 6I_{20}I_{12} + 4I_{30}I_{02} + 9I_{14},$$

$$\langle I_3^2\rangle = I_{30}^2 + 18I_{02}^3 + \tfrac{45}{2}I_{06} + 15I_{12}(I_{30} + 3I_{12}) + \tfrac{9}{2}I_{02}(I_{20}^2 + 2I_{22} + 2I_{02}I_{20} - 9I_{04}) - 18I_{04}I_{20} - \tfrac{9}{2}I_{20}I_{22},$$

$$\langle I_2^3\rangle = I_{20}^3 + 3I_{02}(9I_{04} - 4I_{02}^2 - 12I_{02}I_{20} - I_{20}^2) + 27I_{04}I_{20} + 18I_{22}(3I_{02} + I_{20}), \tag{19}$$

with

$$I_{pq} = \frac{1}{2}\sum_{\alpha=1}^{3} m_\alpha^p \sigma_\alpha^q \quad (I_2 \equiv I_{20}, I_3 \equiv I_{30}). \tag{20}$$

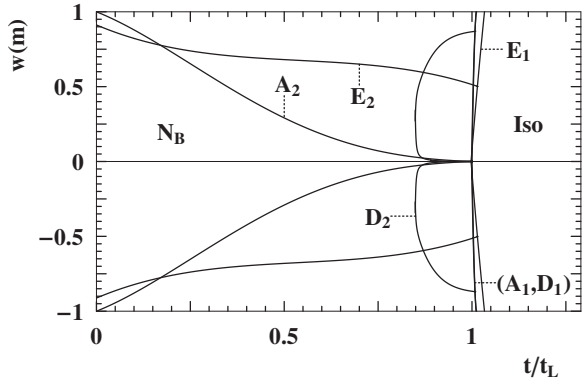

FIG. 3. Phase diagrams for $\sigma_1=\sigma_2$. Diagram labeled A_i corresponds to $\sigma_1=0$ [8], while diagrams D_i and E_i to $\sigma_1=0.15$. Subscript $i=1$ refers to the isotropic (iso)nematics phase transition lines whereas subscript $i=2$ refers to the uniaxial nematic-biaxial nematic (N_B) lines. For diagrams D_i and E_i we took $\tilde{\lambda}=0.99$ and $\tilde{\lambda}=-0.99$, respectively.

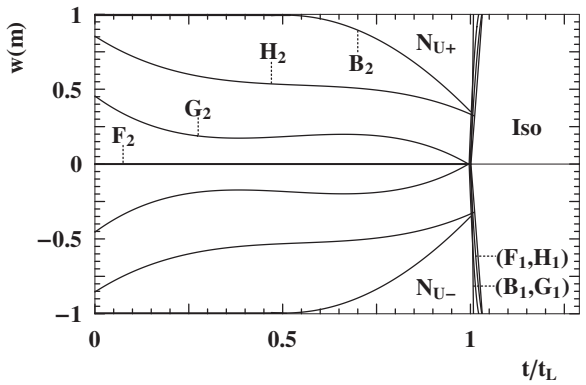

FIG. 4. Phase diagrams for $\sigma_1=0.15$ and $\lambda=0$. Diagram B_i corresponds to $\sigma_2=0$, while diagrams F_i, G_i, and H_i correspond to $\sigma_2=0.15$, 0.1, and 0.05, respectively. Subscript $i=1$ refers to the isotropic (iso)nematics phase transition lines, whereas subscript $i=2$ refers to the uniaxial nematic (N_U+,N_U-)-biaxial nematic lines. The lines for the isotropic-nematic phase transitions occur in the following order (from left to right): B_1, G_1, F_1, and H_1.

Using Eqs. (9) and (18) we find that in the limit of small $\{\bar{\gamma}_i\}$ the bifurcation from isotropic to nematic phase takes place at $t_b=\frac{1}{8}\langle I_2\rangle$. Due to the I_{02} contribution to $\langle I_2\rangle$ ($I_{02}\geq 0$) the bifurcation temperature, t_b, is always greater than the corresponding bifurcation temperature for the monodispersive system with molecules characterized by the average shape parameters $\{m_i\}$. Similar result should hold for the transition temperatures, for they usually follow behavior of t_b.

In the vicinity of the isotropic phase the terms higher than sixth order in $\{\bar{\gamma}_i\}$ can be neglected in the expansion (18). Out of the six terms that are left one can associate $\langle I_3\rangle$ with an effective molecular shape anisotropy of the system in the isotropic phase. The I_{12} term, contributing to $\langle I_3\rangle$ and being of undetermined sign, effectively changes this anisotropy and thus has a profound effect on stability of the biaxial phase. More specifically, as $\langle I_2\rangle \geq I_{20}$ and $\langle I_2^2\rangle \geq I_{20}^2$, for I_{30} and I_{12} of opposite sign with $|I_{12}|<|I_{30}|$ the $\langle I_3\rangle$ coefficient can effec-

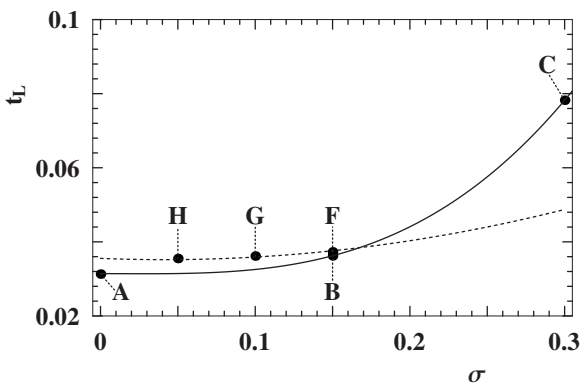

FIG. 5. Isotropic-nematic transition temperature t_L for $w(\mathbf{m})=0$ as a function of σ_1 or σ_2, collectively denoted σ. For continuous line $\sigma=\sigma_1$ with $\sigma_2=0$, whereas for dashed line $\sigma=\sigma_2$, $\sigma_1=0.15$, and $\lambda=0$. Points A, B, and C correspond to $\sigma_1=0$, 0.15, and 0.3, respectively. Points F, G, and H correspond to $\sigma_2=0.15$, 0.1, and 0.05, respectively.

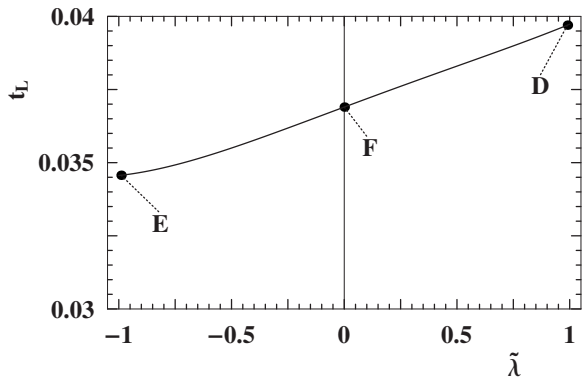

FIG. 6. Isotropic-nematic transition temperature t_L for $w(\mathbf{m})=0$ as a function of $\tilde{\lambda}$ for $\sigma_1=\sigma_2$. Points D, E, and F correspond to $\tilde{\lambda}=0.99$, -0.99, and 0, respectively.

tively be reduced by the shape fluctuations. If, simultaneously, the invariant $\langle I_2 I_3\rangle$ is also reduced by fluctuations, which as we checked is easily achieved in the parameter space, the range of stability of the biaxial phase in $[w(\mathbf{m}), t/t_L]$ space gets enhanced as compared to the case without shape fluctuations. That is, a sufficient condition to observe a constructive role of shape fluctuations in stabilizing the biaxial nematic phase is the simultaneous fulfilment of two inequalities

$$|\langle I_3\rangle| \leq |I_{30}|, \tag{21}$$

$$|\langle I_2 I_3\rangle| \leq I_{20}|I_{30}|. \tag{22}$$

Interestingly, any shape fluctuations about spherically symmetric shape ($m_\alpha=0$) stabilize the biaxial nematic phase of maximal biaxiality ($\langle I_2^n I_3\rangle=0$), without the intermediate uniaxial phase.

Now we turn to detailed analysis of the model. We carried out numerical minimization to determine phase diagrams for a representative set of model parameters. All distinct classes of the diagrams identified are shown in Figs. 2–4. In particular, we found that the class of parameters where the biaxial nematic phase enhances its stability is much more possible than the condition (21) may suggest. However, we are unable to find numerical limitations on the model parameters in a compact form, except for some limiting cases. But even in these limiting cases we recover all observed classes of the phase diagrams. The simplest case occurs when one of the dispersions, say σ_2, vanishes. This corresponds to the Gaussian distribution for μ_1 and μ_3 ($\sigma_1=\sigma_3$), and Dirac delta distribution for μ_2. Phase diagrams, influenced by this polydispersivity, already exhibit quite different topology as compared to the original MR model. This we illustrated in Fig. 2, where diagrams B and C correspond to $\sigma_1=0.15$ and $\sigma_1=0.3$, respectively. Note a considerable enhancement of stability of the biaxial phase along with splitting of the original MR quadruple Landau point into two triple points. The triple points are connected by the line of the first-order transition between the isotropic and biaxial phases. Moreover, as expected, the transition temperature, t_L, of the isotropic-nematic phase transition increases with increasing value of σ_1, Fig. 5.

A subsequent case to consider is the full Gaussian distribution. We limit ourselves to the symmetric distributions with $\sigma_1=\sigma_2$. Now the phase diagrams exhibit yet another topology, which is represented by the diagram D in Fig. 3. Amazingly, there are two triple points and the Landau point on one diagram, and two lines of the direct first-order phase transition between the isotropic and biaxial phases for $|w(\mathbf{m})| \gtrapprox 0.8$. Stable uniaxial phases form two bubblelike islands. As before, the transition temperature, t_L, between the isotropic and nematic phases is higher than that of the MR model and increases with increasing $\tilde{\lambda}$, Fig. 6. Other possible diagrams obtained for this case are shown in Fig. 4. In the diagram F the biaxial phase is practically eliminated being reduced to a line $w(\mathbf{m})=0$. It is interesting to follow reduction of stability of the biaxial phase by comparing diagrams B, H, G, and F, where changes of σ_2 from zero to σ_1, for fixed σ_1, correspond to successive phase diagrams. Numerical estimates of the low-temperature part of the phase diagrams have been checked to stay consistent with asymptotic expansion $\left(\frac{1}{t}\to\infty\right)$ of the self-consistent equations $\{\partial F/\partial\bar{\gamma}_i=0\}$ for $\{\bar{\gamma}_i\}$.

IV. SUMMARY

We have studied the influence of the variable molecular shape anisotropy on stability of the biaxial nematic phase. To make the analysis as simple as possible we generalized the exact mean-field solution obtained by Mulder and Ruijgrok [8] for biaxial molecules to the case when the quadrupole tensor is a dynamical variable. We assumed that at equilibrium, the molecular shape anisotropy can be approximated by the (annealed) distribution, P, of the molecular parameters $\{\mu_\alpha\}$. In the mean-field approximation the natural choice for P, consistent with the maximum entropy principle applied in the isotropic phase, is the two-dimensional Gaussian distribution.

The nonzero second moments of the Gaussian distribution lead to important remodeling of the original MR phase diagram. We observe that polydispersivity changes the range of the stable biaxial phase and that behavior of the system can qualitatively differ from its monodispersive counterpart characterized by the average shape parameters $\{m_i\}$. Generally, the transition between the isotropic and the nematic phases occurs at higher temperatures when molecular shape changes are allowed. The phase diagram is modified, for instance, by showing the quadruple Landau point being split into two triple points connected by a line of first-order transitions between the isotropic and biaxial phases. By comparing diagrams B, D, and E we can conclude that strong correlations between shape fluctuations along the main molecular axes ($|\tilde{\lambda}|\to 1$), or fluctuations along two of the three molecular principal axes lead to a particularly large region of stable biaxial phase. Importantly, fluctuations about isotropic shape give rise to stable biaxial nematic without intermediate uniaxial phase, while fluctuations about fixed $w(m)$, diagram

G, show on the temperature axis two uniaxial phases separated by the biaxial nematic.

In some cases the biaxial phase can be destabilized in the vicinity of the isotropic phase giving only the uniaxial nematic phases and first-order phase transitions between them (class F, Fig. 4). A similar case has recently been observed by Bates [23] in his computer simulation of a generic, flexible V-shaped molecules on a lattice. The only difference between our predictions and that of [23] is that we do not observe a biaxial nematic phase at low temperatures, shown in Fig. 5(a) of [23]. A reason for that is our neglecting of temperature dependence in the isotropic distribution (13) at low temperatures [24]. Clearly, to be consistent with general thermodynamics at $T=0$ the distribution (13) should approach Dirac delta function about m_α. In our studies we have disregarded any temperature dependence in (13), being primarily interested in the system's behavior close to the isotropic phase. However, the diagram predicted in [23] can also be obtained within our model if we replace σ_α by $\sqrt{t}\sigma_\alpha$ in (13). Then the ground state of (9) for $w(\mathbf{m}) \neq \pm 1$ would always be the biaxial nematic phase and, consequently, the phase diagrams of the class F, Fig. 4, would go into generic diagrams found by Bates.

ACKNOWLEDGMENTS

This work was supported by Grant No. N202 169 31/3455 of the Polish Ministry of Science and Higher Education, and by the EC Marie Curie Actions "Transfer of Knowledge," project COCOS (Contract No. MTKD-CT-2004-517186).

[1] M. J. Freiser, Mol. Cryst. Liq. Cryst. **14**, 165 (1971).
[2] L. J. Yu and A. Saupe, Phys. Rev. Lett. **45**, 1000 (1980).
[3] For a comprehensive overview see, e.g., A. M. Figueiredo Neto and S. R. A. Salinas, *The Physics of Lyotropic Liquid Crystals: Phase Transitions and Structural Properties* (Oxford University Press, Oxford, 2005.)
[4] J-F. Li, V. Percec, C. Rosenblatt, and O. D. Lavrentovich, Europhys. Lett. **25**, 199 (1994).
[5] L. A. Madsen, T. J. Dingemans, M. Nakata, and E. T. Samulski, Phys. Rev. Lett. **92**, 145505 (2004).
[6] B. R. Acharya, A. Primak, and S. Kumar, Phys. Rev. Lett. **92**, 145506 (2004).
[7] K. Merkel, A. Kocot, J. K. Vij, R. Korlacki, G. H. Mehl, and T. Meyer, Phys. Rev. Lett. **93**, 237801 (2004).
[8] B. M. Mulder and Th. W. Ruijgrok, Physica A **113**, 145 (1982).
[9] B. Mulder, Phys. Rev. A **39**, 360 (1989).
[10] L. Longa, P. Grzybowski, S. Romano, and E. Virga, Phys. Rev. E **71**, 051714 (2005).
[11] F. Bisi, E. G. Virga, E. C. Gartland, G. De Matteis, A. M. Sonnet, and G. E. Durand, Phys. Rev. E **73**, 051709 (2006).
[12] For a comprehensive review see D. W. Bruce, Chem. Rec. **4**, 10 (2004).
[13] P. H. Nelson, G. C. Rutledge, and T. A. Hatton, J. Chem. Phys. **107**, 10777 (1997).
[14] M. Girardi and W. Figueiredo, Physica A **319**, 421 (2003).
[15] P. S. Christopher and D. W. Oxtoby, J. Chem. Phys. **118**, 5665 (2003).
[16] D. Duque and P. Tarazona, J. Chem. Phys. **107**, 10207 (1997).
[17] For recent references see J. M. Deutsch and M. Warkentin, Phys. Rev. Lett. **95**, 257802 (2005); T. Liu and R. Bundschuh, Phys. Rev. E **72**, 061905 (2005); D. Andelman and J. F. Joanny, Macromolecules **24**, 6040 (1991).
[18] E. F. Gramsbergen, L. Longa, and W. H. de Jeu, Phys. Rep. **135**, 197 (1986).
[19] L. Longa and H. R. Trebin, Phys. Rev. A **42**, 3453 (1990); **39**, 2160 (1989).
[20] C. Itzykson and J.-B. Zuber, J. Math. Phys. **21**, 411 (1980).
[21] G. R. Luckhurst, C. Zannoni, P. L. Nordio, and U. Segre, Mol. Phys. **30**, 1345 (1975).
[22] F. Biscarini, C. Chiccoli, P. Pasini, F. Semeria, and C. Zannoni, Phys. Rev. Lett. **75**, 1803 (1995).
[23] M. A. Bates, Phys. Rev. E **74**, 061702 (2006).
[24] By this we mean that the mean-field theory of the biaxial nematics renders the differences between the fluctuating C_{2v}-symmetric model of Bates and the fluctuating D_{2h}-symmetric quadrupole model of secondary importance. Indeed, take the D_{2h}-symmetric one-particle distribution function as given by Eq. (35) in [10]. Then, the mean-field approximation to the model of Bates leads to an effective D_{2h}-symmetric, mean-field interaction consistent with the one in the curly brackets of Eq. (37) in [10]. Shape fluctuations go into fluctuations in the parameters of the effective potential. Hence, the dipolar effect of the C_2 axis averages out in the D_{2h}-symmetric nematic phase and the symmetry of the fluctuating V-shaped model in the mean-field approximation is effectively that of the fluctuating quadrupole model.